

**NASA  
Technical  
Paper  
2730**


**AVSCOM  
Technical  
Memorandum  
87-B-6**

July 1987

# Preliminary Structural Design of Composite Main Rotor Blades for Minimum Weight

Mark W. Nixon

**NASA**

  
US ARMY  
AVIATION  
SYSTEMS COMMAND  
AVIATION R&T ACTIVITY

**NASA  
Technical  
Paper  
2730**

**AVSCOM  
Technical  
Memorandum  
87-B-6**

1987

# Preliminary Structural Design of Composite Main Rotor Blades for Minimum Weight

Mark W. Nixon

*Aerostructures Directorate  
USAARTA-AVSCOM  
Langley Research Center  
Hampton, Virginia*

**NASA**

National Aeronautics  
and Space Administration

Scientific and Technical  
Information Office

## Summary

A methodology is developed to perform minimum-weight structural design of composite or metallic main rotor blades subject to aerodynamic performance, material strength, autorotation, and frequency constraints. The constraints and load cases are developed such that the final preliminary rotor design will satisfy U.S. Army military specifications. In addition, the methodology uses design variables which can take advantage of the versatility of composite materials. A minimum-weight design is first developed subject to satisfying the aerodynamic performance, strength, and autorotation constraints for all static load cases. The minimum-weight design is then dynamically tuned to avoid resonant frequencies occurring at the design rotor speed.

With this design methodology, three rotor blade designs were developed based on the geometry of the UH-60A Black Hawk titanium-spar rotor blade. The first design is of a single titanium-spar cross section which is compared with the UH-60A Black Hawk rotor blade. The second and third designs use single and multiple graphite/epoxy-spar cross sections, respectively. These are compared with the titanium-spar design to demonstrate weight savings from use of this design methodology in conjunction with advanced composite materials.

## Introduction

Composite rotor blades have demonstrated improvements over metal blades in fatigue strength, damage tolerance, corrosion resistance, and life-cycle costs, as demonstrated in references 1 to 5. However, these improvements were gained with little regard to the tailorability aspects of composite materials. Tailoring is the process of adapting the mass and stiffness characteristics of a composite structure in an effort to improve one or more structural responses. Design methodologies which do not take advantage of composite tailoring may overlook potential advances in blade technology. Additional improvements can be achieved in areas such as weight, frequency placement, and ballistic tolerance provided the blade is designed through use of a methodology capable of exploiting the versatility of composite materials.

A design methodology defines a procedure for obtaining design goals and satisfying design requirements. The procedure is generally based on the minimization of an objective function subject to constraint conditions. An objective function is a mathematical expression of the design goal which is based on one or more design variables. The design variables are changed in a way to achieve the desired design goal.

Constraints are applied so that certain minimum requirements for the blade design are satisfied. Typical constraint conditions utilized in rotor blade design involve aerodynamic performance, material strength, autorotation, and natural frequencies. The aerodynamic performance characteristics of the blade are of primary importance, which usually leads to definition of a fixed external geometry. Constraints should be formulated to assure preservation of the basic aerodynamic geometry to preclude degradation of aerodynamic performance. Structural considerations require adequate blade strength for a defined set of load cases. Any design of rotor blades must also take into account the autorotation capability required for the helicopter. Autorotation capability is primarily a function of the vehicle gross weight, the rotor speed, and the mass moment of inertia of the blades in the rotational plane. The natural frequencies of the blades must be well removed from integer multiples of the forcing frequency at the design rotor speed. Besides the obvious benefit of avoiding destructive resonance, the proper placement of frequencies also tends to increase the blade fatigue life and to improve its vibratory characteristics.

Past works (refs. 6 to 9) on preliminary rotor blade design have focused upon constraint and design variable definition. Minimum-weight rotor blade designs constrained by flutter in hover and by frequency placement were investigated in reference 6. The weight savings were between 3.5 and 9.6 percent of the initial blade weight. The study conducted in reference 6 concluded that greater weight savings would be achieved if there were more design parameters available. Reference 7 formulated an objective function of minimum oscillatory hub shears and hub rolling moments at a specified advance ratio. A by-product of the optimization was a 9- to 20-percent reduction in weight over the initial uniform blade. The weight was probably reduced because the methodology assumed an increase of mass at the blade tip. No constraints related to static strength or deformation were used. Therefore, the final optimized design could be structurally inadequate. Furthermore, tuning mass was added along the outer one-third of the blade, which is not necessarily the optimum position for reducing vibration based on the results of reference 8.

The study conducted in reference 8 investigated the effect of adding a 10-lb mass at various spanwise locations on a UH-60A rotor blade. Dependent upon specific blade properties and flight conditions, the results indicated the most effective position of a tuning mass was at  $0.50R$ . Reference 8 also pointed out that vibration depends on fuselage dynamics, so that a rotor design which is successful on one aircraft may

not be successful on another. These results suggest minimization of hub forces may not be an effective means of vibration reduction in preliminary blade design, especially in cases where fuselage characteristics are unknown. The design methodology developed by reference 9 formulated a two-step optimization procedure in which the objective function was first based on frequency placement with structural constraints. After an optimization was conducted, the objective function was changed to minimum weight with frequency windows used as constraints. Constraints on autorotation and geometry were included in both steps. In one example of reference 9, the weight of a "representative" rotor blade was reduced by two-thirds. However, the strength constraint used by reference 9 was based solely on centrifugal loads, and there was no consideration given to blade deformations. Although the airfoil geometry was fixed in the example, large displacements under realistic flight loads could have severe implications on aerodynamic performance.

References 6 to 9 do not offer a consensus concerning the appropriate objective function or constraints for rotor blade design. In this paper a methodology is described which uses a minimum-weight objective function with a set of constraint conditions developed to obtain acceptable aerodynamic performance, strength, autorotation, and natural frequencies. The method developed herein is unique with respect to its incorporation of U.S. Army military specifications as defined in reference 10 and its use of torsional deformation to define aerodynamic performance constraints. The methodology is also unique in its use of design variables which can exploit the tailorability of composite materials.

Three rotor blade designs are developed with this design methodology. The first design is representative of a UH-60A Black Hawk rotor blade which has a single titanium spar. This first optimized design is compared with the existing UH-60A design to validate the adequacy of the design procedure. The second and third designs use single and multiple graphite/epoxy-spar cross sections, respectively. These designs are compared with the titanium-spar design to demonstrate the weight savings possible from use of composites with minimum-weight design practice as developed in this methodology.

## Symbols

AI	autorotation index
$b$	number of rotor blades
CF	centrifugal force, lb
C.G.	center of gravity

$c$	chord length in.
$E$	extensional modulus
FDVT	frequency design variable tuned
$G$	shear modulus
$hp$	horsepower
$I$	rotational mass moment of inertia, lb-in-s <sup>2</sup>
$I_{\theta}$	mass moment of inertia about elastic axis, lb-in-s <sup>2</sup>
$L_f$	flapwise air load, lb
$l_i$	segment length, in.
$m$	mass, slug
$N_z$	vertical load factor
$n$	number of segments in model
$p(r)$	lift load, lb/in.
$q(r)$	inertial load, lb/in.
$R$	radius, in.
$\bar{R}$	stress interaction ratio
$r$	radial position, in.
SDGW	structural design gross weight
SDVT	static design variable tuned
$T_{PM}$	torque due to propeller moment
$X, Y, S$	laminate strengths in principal material directions, psi
$\theta$	blade pitch angle, rad
$\nu$	Poisson's ratio
$\sigma$	stress, psi
$\Omega$	angular velocity, rad/s
$\dot{\Omega}$	angular acceleration, rad/s <sup>2</sup>
Subscripts:	
$a$	axial
$f$	flapwise
HOGE	hover out of ground effect
$i$	elemental value (refers to segmental value)
1, 2, 12	principal material directions

## Design Methodology

The methodology is divided into seven sections: *Aerodynamic Blade Design, Blade Structural Models,*

*Design Constraints, Design Variables, Load Cases, Minimum-Weight Static Design Procedure, and Dynamic Tuning Procedure.* These sections are covered in detail following the *Overview* section.

## Overview

This section briefly outlines the steps of the design methodology summarized in the flowchart of figure 1. As a starting point, the methodology requires an aerodynamic blade design which defines a basic geometry. A blade structural model is then defined to fit within the aerodynamically defined geometry. Next, design variables are selected with consideration given to both the aerodynamic design and the blade structural model. Numerical values for the constraints and the loads are then defined based on helicopter parameters such as gross weight, number of blades, and rotor speeds. Next, a minimum-weight static design procedure is performed, in which the optimum design variable values are determined. The resulting minimum-weight design is the initial guess for the dynamic tuning procedure. Here, the blade is tuned with the minimum addition of mass required.

## Aerodynamic Blade Design

An aerodynamic design must be developed prior to using the structural design methodology. Parameters such as blade radius, chord length, airfoil contour, twist, and taper are typically defined by an aerodynamic design to form the external geometry of the blade. The external geometry can be thought of as a “glove” within which the structural design must fit.

## Blade Structural Models

The design methodology requires two types of blade models, a cross-section model and a finite-element model. A finite-element beam model is used as a basis for structural analysis of the blade. The beam model consists of a series of beam segments connected at spanwise grid points. Each segment contains equivalent beam properties such as bending stiffnesses, extensional stiffness, torsional stiffness, and mass. These properties are constant along a single beam segment, but may vary between segments, thus forming a step function of beam property distributions along the blade span. Displacements (translational and rotational) and beam forces (shears and moments) resulting from any applied loads are computed at the grid points.

Cross-section models are used to generate the equivalent beam properties for each segment of the

beam model. The cross-section model is a representation of the internal structure, which is comprised of several structural and nonstructural components. These components generally consist of one or more spars, a leading-edge weight, a core, and a skin. The cross-section design is based upon experience, manufacturability, geometrical constraints, and nonaerodynamic considerations such as ballistic tolerance. Cross-section models are also used to calculate stresses on the structural components based upon beam forces calculated from the finite-element analysis. In this manner, each component of a cross section can be modified individually.

## Design Constraints

The constraints used in this design methodology can be categorized as aerodynamic performance, material strength, autorotation, and frequency. The aerodynamic performance characteristics required for the blade are initially satisfied by an aerodynamic design. To guarantee that these characteristics are maintained during the static structural design, a constraint must be imposed which limits blade deformations. Flapwise and in-plane bending deformations are readily satisfied because of the inherently high bending stiffness of composite blades. However, this is not the case with twist deformation. Therefore a constraint is applied to limit rotor twist deformation to ensure that aerodynamic performance is not degraded. The major contribution to twist deformation comes from centrifugal flattening, or “propeller moment,” which tends to decrease any built-in blade twist. A loss of built-in twist increases the horsepower required for forward flight, thereby degrading aerodynamic performance. The allowable magnitude of twist deformation depends on the helicopter system, but typically ranges from 0.5° to 5.0° measured root to tip.

The material strength constraint imposed in the design process is based upon the material strength design allowables. All stresses in the blade structure must be less than the design allowable stress of the material for all load cases. To account for stress interactions, a Tsai-Hill failure criterion (ref. 11) is calculated based on the material limit allowable stresses. The governing equation is given by

$$\bar{R} = \sqrt{\frac{\sigma_1^2}{X^2} - \frac{\sigma_1\sigma_2}{X^2} + \frac{\sigma_2^2}{Y^2} + \frac{\sigma_{12}^2}{S^2}} \quad (1)$$

The quantity  $1 - \bar{R}$  is a material strength margin of safety which must be greater than zero for a feasible design.

The autorotation constraint pertains to maintaining the mass moment of inertia of the rotor in the rotational plane at an acceptable level. Autorotation capability is actually a function of design gross weight and rotor aerodynamics as well as the rotor system mass moment of inertia. However, the aerodynamics have been previously defined as required for starting this methodology, and design gross weight is typically the first parameter defined for any helicopter system. Thus, the only variable left to achieve a satisfactory autorotation capability is mass moment of inertia. The equation used to calculate the required rotor inertia  $I$  is given by reference 12 as

$$AI = \frac{I\Omega^2}{1100hp_{HOGE}} \quad (2)$$

where AI is an autorotation index of no less than 1.7 for single rotor aircraft.

The dynamic constraint requires natural frequencies of the blade to avoid integer multiples of the forcing frequency by at least a margin of  $\pm 0.2$  times each multiple. This is done to avoid resonance conditions which could damage or destroy the rotor system. There is difficulty in defining the direction of change required to satisfy the frequency constraints because these constraints can be satisfied with either an increase or a decrease of the frequency in question. Furthermore, the frequencies do not all move in the same direction for a given change of mass or stiffness. If the frequency constraints are applied to a poor design, they might prevent a good design from occurring because the design variables will be restricted so that the constraint is satisfied. Better designs might exist with a set of design variables which would move through three or four sets of frequency constraints. Because of these reasons, the frequency constraints are imposed after a minimum-weight static design has been developed. Thus, the frequency constraints (one for each mode considered) are not specified until the design variables are stabilized with respect to aerodynamic performance, material strength, and autorotation considerations. From this point, only slight modifications in the stiffnesses and the weight distributions may be required to satisfy the frequency constraints. If not, the design variables can be changed such that the new set of variables will have maximum influence on frequency shifts with minimum influence on the previous optimum design.

### Design Variables

Design variables are used in the iterative design process to make changes in both structural and non-structural parts of the rotor blade. The number of

design variables necessary to define a component of the blade depends on assumptions made for the basic cross-section design. For example, the designer may assume a blade will have a circular spar of a specific diameter based on the maximum thickness of the airfoil. This assumption eliminates spar location and geometry as design variables. Thus, increasing the number of assumptions in the basic design reduces the number of design variables required. Upper and lower bounds for the magnitudes of each design variable are defined through physical limitations and through initial geometries set by aerodynamic design. Engineering judgment must be used to decide which variables are pertinent to the objective function and what range of values is to be considered for each.

### Load Cases

The required static load cases are outlined in reference 10 and are discussed in detail in reference 12. They are described below in terms of flapwise, in-plane, torsional, centrifugal, and nonflight loads. The method of calculating the load magnitudes and distributions for each case are covered in this section.

**Flapwise loads.** Flapwise load magnitudes are defined as a function of load factors  $N_z$  and structural design gross weight (SDGW) of the total helicopter system. The critical flapwise load factors used under current structural design requirements range from  $-0.5$  to  $3.5$  for most military helicopters. The total flapwise load is equal to  $N_z$  times the structural design gross weight of the system. Thus, the magnitude of the flapwise airload  $L_f$  carried by one blade in a rotor system of  $b$  blades is given by reference 10 as

$$L_f = (N_z)(SDGW)/b \quad (3)$$

Distribution of the load, which is a function of azimuth position, is representative of actual air loads the blade produces in forward flight. The actual air load is scaled proportionally at each spanwise position until the total load equals the required load  $L_f$ . The actual blade air loads are obtained from flight data, from wind tunnel data, or through a computer-simulated aerodynamic performance analysis such as C81 (ref. 13).

**In-plane loads.** The in-plane loads are based on two cases of shaft torque transmission from the power plant. One case emanates from a power increase with subsequent rotor acceleration. Here, a shaft torque is transmitted through the hub, creating an in-plane moment at the blade root. The limit root in-plane

moment  $M_E$  is given by reference 10 as

$$M_E = \frac{1.5M_T}{b-1} \quad (4)$$

where  $M_T$  is the torque developed at the military power rating of the power plant. The second case requires that twice the maximum braking torque be equally transmitted to all blades. The root moment for both cases is balanced by an inertial force distribution developed along the blade span such that

$$M_E = \sum_{i=1}^n m_i r_i^2 \dot{\Omega} \quad (5)$$

where  $i$  refers to the  $i$ th blade segment of the beam model. After solving for  $\dot{\Omega}$ , the in-plane inertial loads  $q_i(r)$  for the  $i$ th segment can be written as

$$q_i(r) = \frac{m_i r_i \dot{\Omega}}{l_i} \quad (6)$$

**Torsional loads.** There are two basic contributions to the static torsional loads of a rotor blade. The first is because of the aerodynamic pitching moment of an airfoil section, and the second is because of the propeller moment caused by centrifugal forces. Aerodynamic pitching moment is a function of chord, air density, and Mach number. Since the Mach number is itself a function of several flight variables, it is helpful to choose a standard load case. The flight condition used to define the pitching moments in this methodology is design velocity at 4095 ft on a 95°F day. The second torsional load contribution is from the propeller moment caused by centrifugal forces. Mass of the blade cross section is distributed both forward and aft of the elastic axis, creating separate centrifugal force vectors which can be resolved into axial and chordwise components as described in reference 14. If the masses are moved out of the rotational plane, as occurs with pitch and twist, the chordwise components produce a moment couple which attempts to flatten the mass back into the rotational plane. This flattening effect has given rise to use of the term "centrifugal flattening." Since rotor blades generally have a built-in twist, there will always be a part of the blade in which the propeller moment can be significant. The torsional loads produced here are proportional to centrifugal force, root angle of attack, and rotor twist (ref. 14) such that

$$T_{PM_i} = I_{\theta_i} \Omega^2 \theta_i \quad (7)$$

The maximum propeller moment occurs at maximum rotational velocity with maximum root angle

of attack for forward level flight. The propeller moment and pitching-moment contributions are combined into one torsional load case.

**Centrifugal loads.** Rotation of the blades creates centrifugal forces which act in the axial direction unless the blade is coned or deformed as a result of other loads. When flapwise loads are applied to a rotating rotor system, the blades both cone and deform in the direction of the load. This creates axial  $(CF_i)_a$  and flapwise  $(CF_i)_f$  components of centrifugal force on the  $i$ th blade segment, and these components oppose the applied loads as shown in figure 2. In the in-plane load case shown in figure 3, an in-plane distributed inertial load  $q(r)$  creates a lag condition. Lead-lag rigid body displacements resulting from the inertial load do not create opposing centrifugal force components because the centrifugal force vector acts along the C.G. axis of the blade. Only deformation can create opposing centrifugal force components for the in-plane case. The deformed blade would have a nonlinear C.G. axis which alters the path of the centrifugal force vector with respect to the local blade segment. However, in-plane deformations are generally negligible because of the high in-plane stiffness which is characteristic of rotor blades.

The maximum centrifugal loads correspond to the maximum rotor rotational velocity. However, the centrifugal loads are combined with the flapwise, in-plane, and torsional load cases as opposed to being applied as a separate load case. The magnitude and distribution of the centrifugal load in each case are governed by the equation (ref. 14)

$$CF_i = m_i r_i \Omega^2 \quad (8)$$

where  $i$  refers to an individual blade segment of the beam model.

**Nonflight loads.** The last load case covers aspects of nonflight loads. Reference 10 requires that an articulated rotor blade be designed for a static load equal to its weight multiplied by a limit load factor of 4.67. Reference 12 determines that this load case covers other adverse conditions such as ground handling, stop-banging, turning the rotor at low speed in a strong wind, and the condition in which a helicopter with an untethered rotor is in the vicinity of an operating helicopter. For this case, the blade is assumed to be cantilevered at the blade stops and under no rotational effects.

## Minimum-Weight Static Design Procedure

Aerodynamic design, basic blade models, load cases, design variables, and constraint conditions are defined prior to initiating the minimum-weight static design procedure. With the information formulated thus far, it is possible to formulate a fully automated optimization analysis. However, the procedure developed to minimize the objective function is a "hand-worked" solution. This procedure works well for cases in which the number of design variables are few. At the preliminary design level, problems with only two or three design variables can generally be devised through the appropriate assumptions. The values of the design variables which produce a minimum of the objective function while satisfying the constraints can be graphically determined.

The minimum-weight static design procedure is an iterative procedure which consists of a series of steps as illustrated in the flowchart of figure 4. The initial magnitudes of the design variables are selected. The blade properties at each spanwise section are then computed. An analysis of the blade is performed for each of the previously described load cases, and the resulting deformations and stresses are calculated. Constraint conditions are then evaluated based on those results. Stress and deformation trends are established for each design variable by repeating the analysis for several magnitudes of one design variable. This defines a design space within which the constraint conditions are satisfied. On each iteration the magnitudes of the design variables are modified to satisfy all constraint conditions simultaneously. Once the design space is established the minimum-weight design can be determined through the relations between design variables and the resulting blade weight.

## Dynamic Tuning Procedure

Although the design space developed for the static case contains a minimum-weight design, the final minimum-weight design cannot be determined without an assessment of natural frequencies. Frequency constraints can now be added because the proximity of the structural design variables are established. The natural frequencies of the modes of the static design are calculated, and the target frequencies are selected based on these results. The modifications necessary for dynamic tuning may require use of additional design variables other than those used in the static design. In the frequency tuning process, if the static minimum-weight design is altered, then the final design must be checked to ensure its validity with respect to strength. If the additional design variables

are such that changes to them could affect the previously established static design, then the final optimized design must be structurally validated with the static analysis. The final design has the minimum total blade weight while simultaneously satisfying all constraint conditions.

## Applications

This section describes three example rotor blade designs which were developed with the previously described design methodology. All three designs are based on the UH-60A Black Hawk titanium-spar blade. The first design case is for a single titanium-spar cross section. This design was conducted to validate the present design methodology. The second and third cases have T300/5208<sup>1</sup> graphite/epoxy spars in single-spar and multispar cross sections, respectively. The composite designs are compared with the metallic-spar design to demonstrate potential weight savings obtained from use of the design methodology in conjunction with composite materials.

### Single Titanium-Spar Cross Section

A titanium-spar blade design was developed with the design methodology described in this paper. The cross-section model is based on the actual UH-60A rotor blade with identical skin, core, trailing-edge tab, leading-edge weight, and spar coordinates. Only the spar thickness is used as a design variable. The beam model representation of the blade uses a rectangular planform similar to the UH-60A planform, but without any tip sweep.

The aerodynamic performance constraint is based on the maximum allowable twist deformation developed from aerodynamic design data. The aerodynamic data are obtained for a typical rectangular planform blade from a computer-simulated aerodynamic performance analysis (Program C81, ref. 13). The horsepower required for steady level flight is related to blade twist deformation in figure 5. With the assumption of a maximum allowable increase in horsepower required of 2.0 percent, total twist deformation must remain under 3.1°. A maximum twist deformation of 3.1° is used as the aerodynamic performance constraint in the design methodology. The structural constraint requires that the calculated stresses do not exceed the allowable material strength. Material properties for titanium are listed

---

<sup>1</sup> T300 graphite fibers are manufactured by Union Carbide Corp.; 5208 epoxy resin is manufactured by Narmco Materials, Inc.



in table I. The material strength is assessed by use of a Tsai-Hill failure criterion and an associated margin of safety as described previously. The margin of safety must be greater than zero to satisfy the material strength constraint. The autorotation capability is assumed to be the same for this design as it is for the UH-60A. Autorotation is satisfied by requiring the mass moment of inertia to be identical to that of the UH-60A rotor system, which is 19000 in-lb-s<sup>2</sup> per blade.

### Single Composite-Spar Cross Section

A second design was developed with a single graphite/epoxy D-spar. Material properties of the T300/5208 composite are presented in table I. The blade models and associated design assumptions used in the composite design are the same as those used for the metallic spar except for the spar material. Thickness and ply orientation of the composite spar are used as design variables. The plies of the spar are assumed to consist of only 0° and ±45° angles symmetrically built up. Thus, the ply orientation design variable is the percentage of ±45° plies in the laminate. The remaining plies of the laminate are understood to be oriented at 0°. Assumptions for twist deformation limit, material strength, and mass moment of inertia are the same as those used for the metallic-spar design.

### Multiple Composite-Spar Cross Section

A third design was developed which used four graphite/epoxy circular tube spars. The beam model used in this design process is the same as those described previously. However, the cross section is different and is illustrated in figure 6. Thickness and ply orientation of the composite spars are again used as design variables, with the added assumption that all four spars are identical except for their diameters. The plies of the spar are again assumed to consist of only 0° and ±45° angles symmetrically built up. The diameter of the spars varies such that each spar is inscribed within the airfoil geometry. From a stability point of view, a mass center forward of 0.25c is generally favorable. Thus, leading-edge weights are added to maintain a C.G. location of 0.24c.

## Results and Discussion

### Single Titanium-Spar Cross Section

The single titanium-spar cross section and beam models described previously were used in the design analysis to determine the minimum-weight design.

Figure 7 is a graph of the change in material strength margin of safety ( $1 - \bar{R}$ ) as a function of spar thickness. From this graph the spar thickness must be at least 0.102 in. thick to satisfy the material strength constraint. The autorotation capability constraint is satisfied within the analysis through choice of the tip mass to produce the required mass moment of inertia. The tip mass required to maintain autorotation capability changes as a function of spar thickness. The twist deformation for various spar thicknesses is illustrated in figure 8. Herein, all the spar thicknesses which satisfy the strength constraint also satisfy the twist deformation constraint. The minimum-weight design corresponds to the minimum spar thickness, which is 0.102 in. The minimum spar thickness of this design produces a total blade weight of 189 lb as determined from figure 9.

Before a comparison with the UH-60A blade can be made, the design must be dynamically tuned. The forcing frequencies corresponding to the design rotor speed of the UH-60A are listed in table II. This table also shows the frequency regions which the modes considered must avoid to satisfy the 0.2 rev<sup>-1</sup> constraint. The modes considered in this design are first flapwise and in-plane bending, first torsion, and second and third flapwise bending. Figure 10 shows the natural frequency changes with respect to spar thickness for these modes. The minimum spar thickness needed to satisfy the dynamic constraints is 0.130 in., which corresponds to a blade weight of 207 lb. The actual UH-60A titanium spar is 0.135 in. thick, producing a 210-lb blade. The titanium-spar design is only 3 lb different from the actual UH-60A blade, a result demonstrating that the mechanics of the design methodology can produce blade designs similar to conventional design processes. The only significant difference in modal frequencies between the actual UH-60A blade and the titanium-spar design is the frequency of the torsional mode. This difference is attributed to the chordwise distribution of the tip weight, which is lumped at the chordwise C.G. in the titanium-spar design.

### Single Composite-Spar Cross Section

The design procedure was performed for the single composite-spar model with the assumptions described previously. The graph in figure 11 shows material strength margin of safety as a function of spar thickness for different percentages of ±45° plies. There is a different spar thickness required to satisfy the strength constraint for each ply layup. The twist deformation for the load cases considered is also plotted as a function of spar thickness and percentage of ±45° plies in figure 12. There is a different

minimum spar thickness required to satisfy the maximum twist deformation of  $3.1^\circ$  for each ply layup. The combinations of the design variables required to satisfy both the aerodynamic performance and strength constraints are plotted in figure 13. Figure 13 illustrates the boundaries of the design variables for both constraint conditions simultaneously, thus defining a feasible design region. The intersection of the boundaries corresponds to the minimum-weight static design (i.e., minimum spar thickness), which is approximately 0.105 in. thick with 20 percent  $\pm 45^\circ$  plies. The single composite-spar blade weighs 158.8 lb prior to being dynamically tuned.

The single composite-spar design is dynamically tuned with two different methods. In the first method, the same design variables used in the static design are used to tune the blade. The feasible design space shown in figure 13 is subsequently modified by the frequency constraints of the pertinent modes, creating the new design space shown in figure 14. Here, all the constraints— aerodynamic performance, strength, autorotation, and frequency— are satisfied simultaneously. The minimum-weight design found in the new design region has a 0.170-in.-thick spar with 35 percent  $\pm 45^\circ$  plies and weighs 169.5 lb, 10.7 lb more than the untuned version.

The second method used to tune the single composite-spar design is with a new set of frequency design variables. Nonstructural "tuning" weight and in-plane stiffness of the untuned blade are used as the frequency design variables. These design variables are chosen because they both have a significant impact on natural frequencies but may not significantly alter the structural design. A finite-element beam model was developed to calculate the blade frequency sensitivity to selected nonstructural tuning masses and in-plane stiffness. Tuning masses are located at five radial beam stations, while in-plane stiffness is assumed to change uniformly over the span. The dynamically tuned blade requires a total weight increase of only 3.8 lb, bringing the total weight to 162.6 lb.

The weight distributions of the three versions of the single composite-spar design—untuned, static design variable tuned (SDVT), and frequency design variable tuned (FDVT)—are shown in figure 15. It is easy to see where the weights have been increased or decreased in a lumping fashion for the FDVT design. This is opposite from the SDVT version, which has a constant weight increase from the untuned blade. The constant weight increase is created by the earlier design assumption of constant spar thickness over the blade span. The in-plane stiffnesses of the three versions of the single composite-spar design are shown in figure 16. Both the SDVT and FDVT designs use a

stiffness increase to achieve desired frequencies. The FDVT stiffness is constant over the design range because stiffness change is assumed to occur uniformly.

The bar graph of figure 17 depicts the frequencies of the five modes considered for each design along with the resonant frequency avoidance ranges. The main difficulty in tuning the single composite-spar design is encountered with the first elastic flapwise mode. This frequency is the most difficult to change because (1) the lower frequency modes require the greatest mass or stiffness change for a desired frequency shift, and (2) the geometry of the airfoil makes it difficult to modify flapwise stiffness without significantly changing the structural design variables.

### Multiple Composite-Spar Cross Section

The design procedure was performed for the multiple composite-spar models described previously. Figure 18 shows material strength margin of safety as a function of spar thickness for different percentages of  $\pm 45^\circ$  plies. As is the case for the single-spar designs, there is a different spar thickness required to satisfy the strength constraint for each ply layup. The twist deformation for the load cases considered is also plotted as a function of spar thickness and percentage of  $\pm 45^\circ$  plies in figure 19. Here, there is a unique spar thickness required to satisfy the maximum twist deformation of  $3.1^\circ$  for each ply layup. The combinations of the design variables required to satisfy both the aerodynamic performance and strength constraints are plotted in figure 20. This graph illustrates the boundaries of the design variables for both constraint conditions simultaneously, thus defining a feasible design space as indicated. The intersection of the boundaries corresponds to the minimum-weight static design (i.e., minimum spar thickness), which is approximately 0.190 in. thick with 21 percent  $\pm 45^\circ$ . The multiple composite-spar blade weighs 164.6 lb prior to the dynamic tuning procedure.

The multiple composite-spar design is dynamically tuned with the FDVT tuning method. The dynamically tuned blade requires a total weight increase of 17.4 lb, bringing the total weight to 182.0 lb.

The final weight distributions, flapwise stiffnesses, and in-plane stiffnesses for the tuned and untuned versions of the multiple composite-spar design are shown in figures 21, 22, and 23. The weight additions for the tuned blade are again lumped, but not in the same manner as was the case for the single composite-spar design. The flapwise and in-plane stiffnesses are both decreased in the dynamic tuning procedure. The modal frequencies of the two versions of the multiple composite-spar design are plotted in

figure 24. As is the case with the single-spar design, the first elastic flapwise mode frequency shift requires the greatest blade modifications. In the multispar case, the decrease of the first elastic flapwise mode frequency brought the first elastic edgewise modal frequency down into an avoidance range. Moving this frequency out of the avoidance range requires a large decrease in in-plane stiffness. Nonstructural masses are used to decrease the first flapwise frequency while at the same time increasing the second flapwise frequency out of a frequency avoidance range.

## Design Comparisons

Table III summarizes the final results of the three blade designs. The single titanium-spar design is within 2 percent of the weight of the actual UH-60A blade. These results suggest that the design methodology proposed herein will produce results consistent with conventional design practices. Two single composite-spar designs resulted in blade weight savings of 17.9 and 21.3 percent compared with the single metallic-spar design. The design which demonstrates 21.3-percent weight savings is produced with the FDVT procedure with nonstructural mass and in-plane stiffness design variables. This process seems to have the greatest potential for producing minimum-weight blade designs. The reason this method is better is because it can take advantage of additional design variables over those used in the structural design. The multiple composite-spar design is 12.1 percent lighter than the single metallic-spar design; however, it is 11.7 percent heavier than the comparably designed single composite-spar design. Although ballistic tolerance was not accounted for as a constraint, the multispar designs are inherently more ballistically tolerant than single-spar designs. Thus, if ballistic tolerance is considered in the design, the multispar design will probably have the minimum weight of all designs considered.

## Concluding Remarks

A methodology was developed to design main rotor blades for minimum weight subject to aerodynamic performance, material strength, autorotation, and frequency constraints. Three designs based on the aerodynamics of the UH-60A rotor blade were developed to demonstrate the design methodology. The first design represented a single titanium-spar UH-60A type of cross section to validate the methodology. The results demonstrated that the mechanics

of the design methodology can produce blade designs similar to those produced with conventional design procedures. The second design used a single graphite/epoxy spar with design variables of spar thickness and ply orientation. A significant weight savings of 21.3 percent was achieved over the metallic design. Lastly, a design with four graphite/epoxy spars was developed. Assumptions were made to reduce the design variables to the same ones used in the single composite-spar design. The resulting multispar blade was 12.1 percent lighter than the metallic design but was 11.7 percent heavier than the single composite-spar design. These results suggest that, for the constraint conditions considered, multispar designs may in general produce heavier rotor blades than single-spar designs.

NASA Langley Research Center  
Hampton, VA 23665-5225  
May 27, 1987

## References

1. Holmes, R. Doug: S-Glass-Reinforced Plastic Adopted for Helicopter Rotor Blades. *SAMPE Q.*, vol. 7, no. 1, Oct. 1975, pp. 28-41.
2. McCaskill, O. K., Jr.: Composite Applications at Bell Helicopter. SAE Tech. Paper Ser. 790578, Apr. 1979.
3. Maloney, Paul F.: Composite Rotors—An Evolving Art. *ManTech J.*, vol. 3, no. 4, 1978, pp. 17-21.
4. Lofland, R. A. "Dick": Advanced Composites Structures at Hughes Helicopters, Inc. *Material & Process Advances '82*, Volume 14 of National SAMPE Technical Conference, Soc. Advancement of Material and Process Engineering, c.1982, pp. 521-528.
5. Ray, James D.: Composites Important to Black Hawk. *ManTech J.*, vol. 3, no. 4, 1978, pp. 32-36.
6. Bielawa, Richard L.: Techniques for Stability Analysis and Design Optimization With Dynamic Constraints of Nonconservative Linear Systems. AIAA Paper No. 71-388, Apr. 1971.
7. Friedmann, P. P.; and Shanthakumaran, P.: Aeroelastic Tailoring of Rotor Blades for Vibration Reduction in Forward Flight. *A Collection of Technical Papers, Part 2: Structural Dynamics—AIAA/ASME/ASCE/AHS 24th Structures, Structural Dynamics and Materials Conference, 1983*, pp. 344-359. (Available as AIAA-83-0916.)
8. Blackwell, R. H., Jr.: Blade Design for Reduced Helicopter Vibration. *American Helicopter Soc. J.*, vol. 28, no. 3, July 1983, pp. 33-41.
9. Peters, David A.; Ko, Timothy; Korn, Alfred; and Rossow, Mark P.: Design of Helicopter Rotor Blades for Desired Placement of Natural Frequencies. 39th Annual Forum, American Helicopter Soc., 1983, pp. 674-689.
10. *Military Specification—Structural Design Requirements, Helicopters*. MIL-S-8698, Apr. 20, 1981.

11. Jones, Robert M.: *Mechanics of Composite Materials*. Scripta Book Co., c.1975.
12. *Engineering Design Handbook, Helicopter Engineering. Part One—Preliminary Design*. AMCP 706-201, U.S. Army, Aug. 1974. (Available from DTIC as AD A002 007.)
13. Van Gaasbeek, J. R.: *Rotorcraft Flight Simulation, Computer Program C81. Volume II—User's Manual*. USARTL-TR-77-54B, U.S. Army, Oct. 1979. (Available from DTIC as AD A079 632.)
14. Bramwell, A. R. S.: *Helicopter Dynamics*. John Wiley & Sons, Inc., c.1976.

Table I. Properties for Materials Used in Example Designs

Property	Titanium	T300/5208 Gr/Ep
$E_{11}$ , psi $\times 10^{-6}$ . . . . .	16.0	21.3
$E_{22}$ , psi $\times 10^{-6}$ . . . . .	16.0	1.6
$G_{12}$ , psi $\times 10^{-6}$ . . . . .	6.2	0.9
$\nu_{12}$ . . . . .	0.31	0.28
$X$ , ksi . . . . .	120	211
$Y$ , ksi . . . . .	120	6.1
$S$ , ksi . . . . .	76	13.8

Table II. Integer Multiples of Forcing Frequency and Associated Avoidance Ranges

Integer multiple, rev <sup>-1</sup>	Frequency, Hz	Avoidance range, Hz
1	4.38	3.50–5.26
2	8.78	7.90–9.66
3	13.15	12.27–14.03
4	17.53	16.65–18.40
5	21.92	21.04–22.79
6	26.30	25.42–27.18
7	30.68	29.80–31.56
8	35.06	34.18–35.93
9	39.45	38.57–40.32
10	43.83	42.95–44.71

Table III. Final Design Features of Example Blades

Parameter	Actual UH-60A	Single spar, tuned	Single spar (SDVT)	Single spar (FDVT)	Multispar, tuned
Spar material . . . . .	Ti	Ti	Gr/Ep	Gr/Ep	Gr/Ep
Spar thickness, in. . . . .	0.135	0.130	0.170	0.105	0.210
$\pm 45^\circ$ plys in layup, percent . . . . .			35	20	21
Total blade weight, lb . . . . .	210	207	170	163	182
1st flapwise mode, Hz . . . . .	12.7	11.5	12.2	12.2	11.8
2nd flapwise mode, Hz . . . . .	24.1	20.6	19.4	18.4	22.8
3rd flapwise mode, Hz . . . . .	34.6	31.8	36.0	37.1	33.8
1st in-plane mode, Hz . . . . .	20.6	17.6	23.0	23.4	20.7
1st torsion mode, Hz . . . . .	17.5	28.1	21.4	16.8	15.9
Material strength margin $1-\bar{R}$ . . . . .		0.103	0.111	0	0
Twist deformation, deg . . . . .		0.92	1.42	2.55	2.61

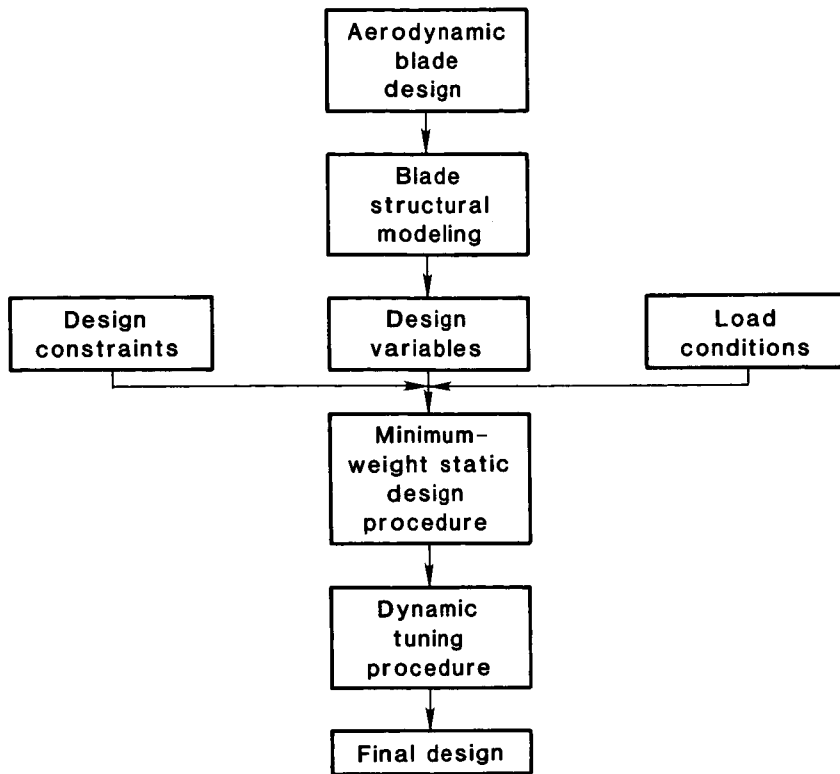


Figure 1. Flowchart of design methodology.

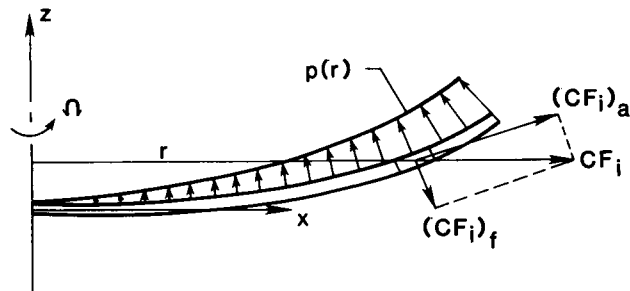


Figure 2. Interaction of flapwise and centrifugal loads acting on rotor blade model.

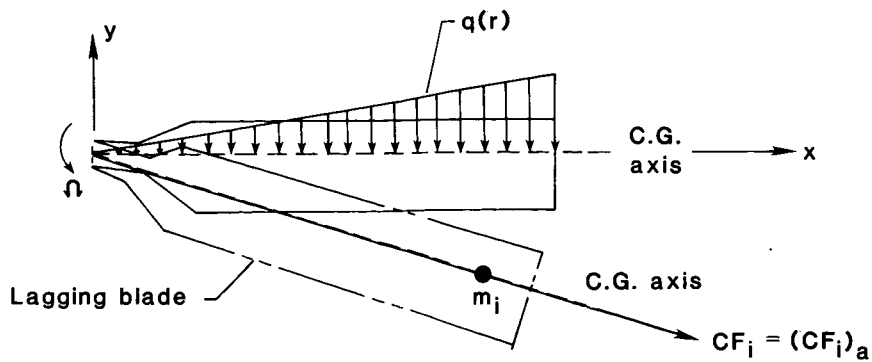


Figure 3. Interaction of in-plane and centrifugal loads acting on a rotor blade model.

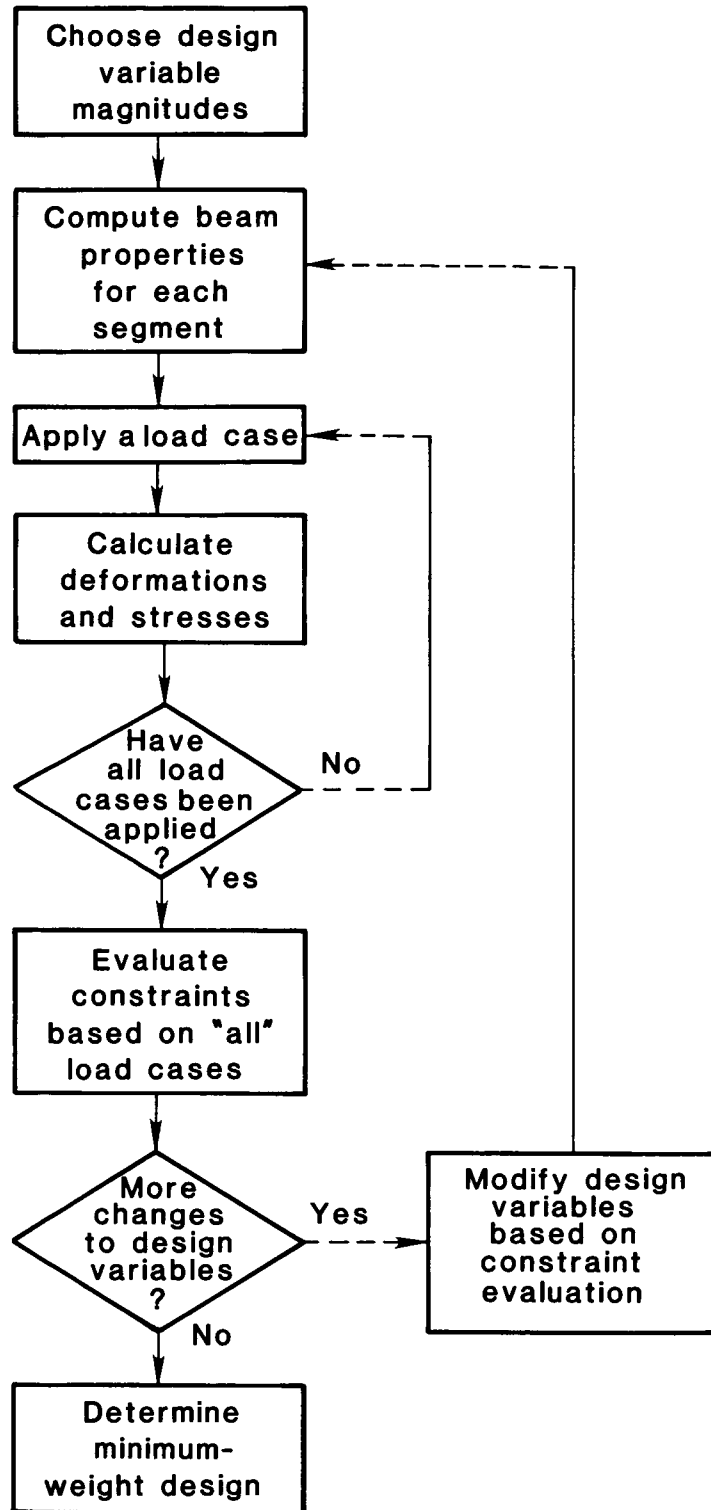


Figure 4. Minimum-weight static design procedure.



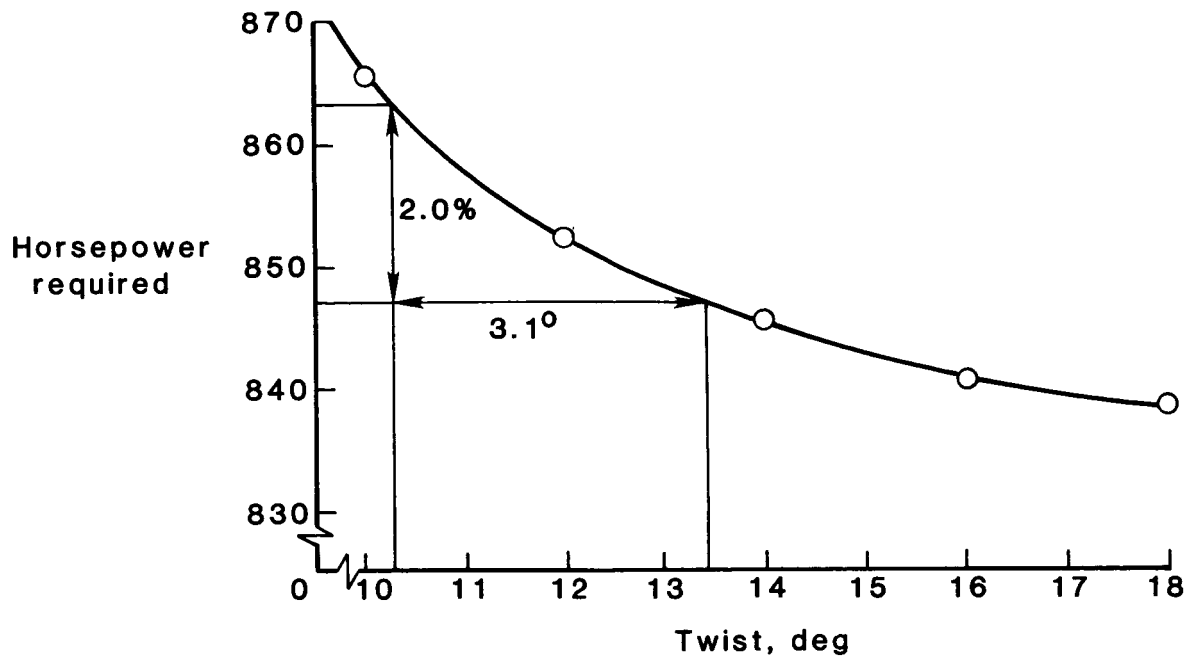


Figure 5. Horsepower required for steady level flight as function of blade twist.

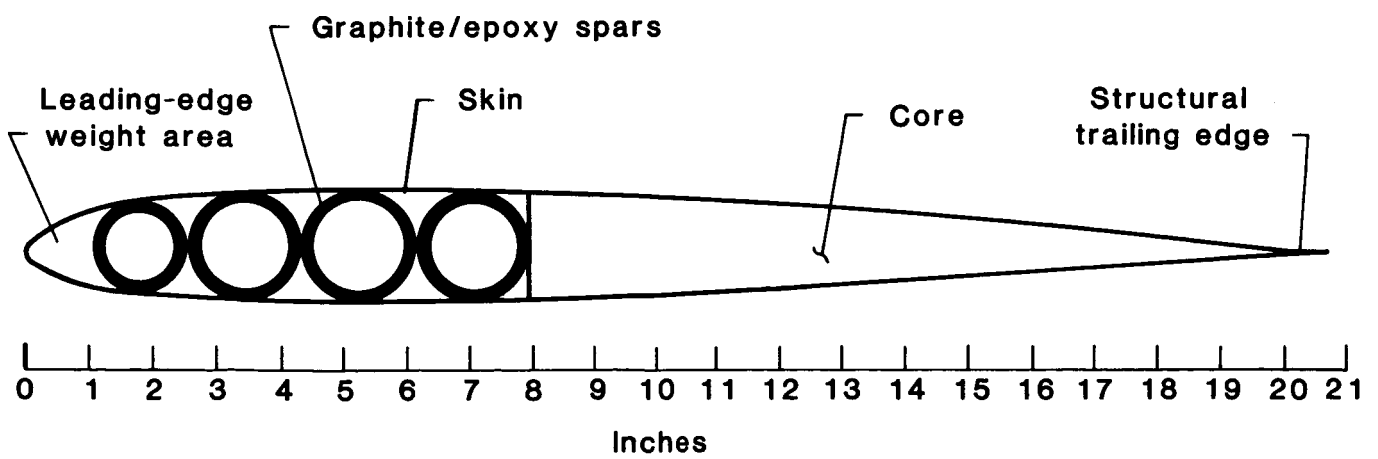


Figure 6. Cross-section design for four-spar blade.

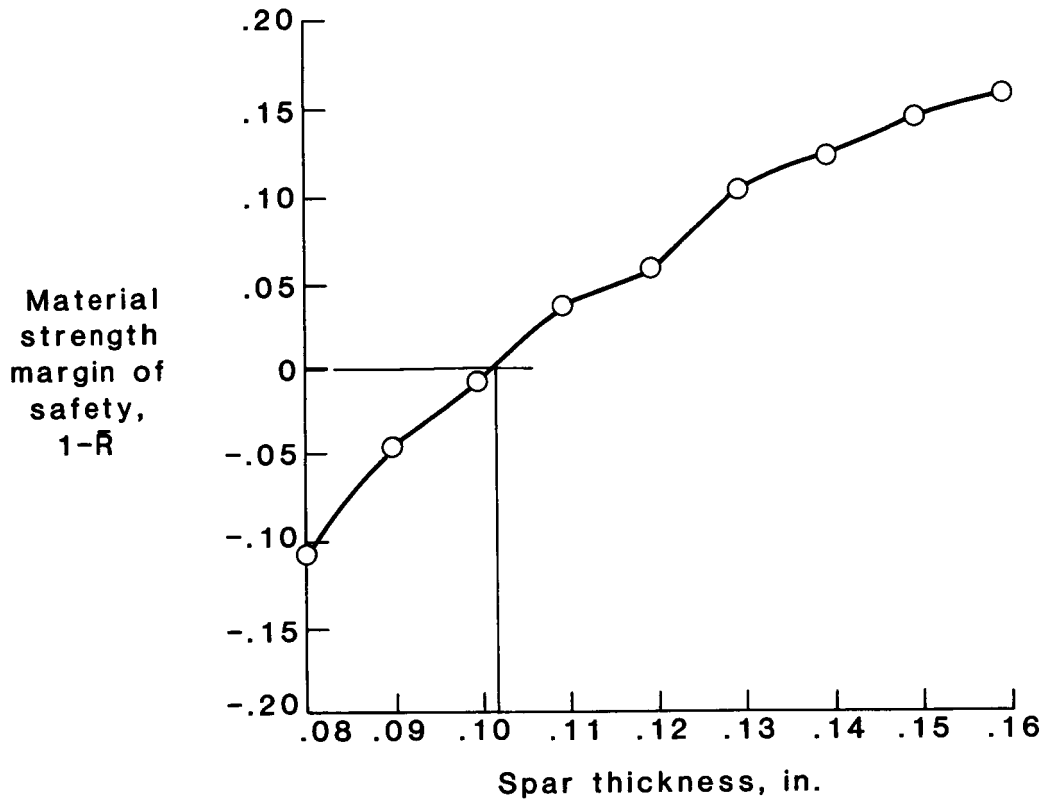


Figure 7. Material strength margin of safety as function of spar thickness for titanium-spar design.

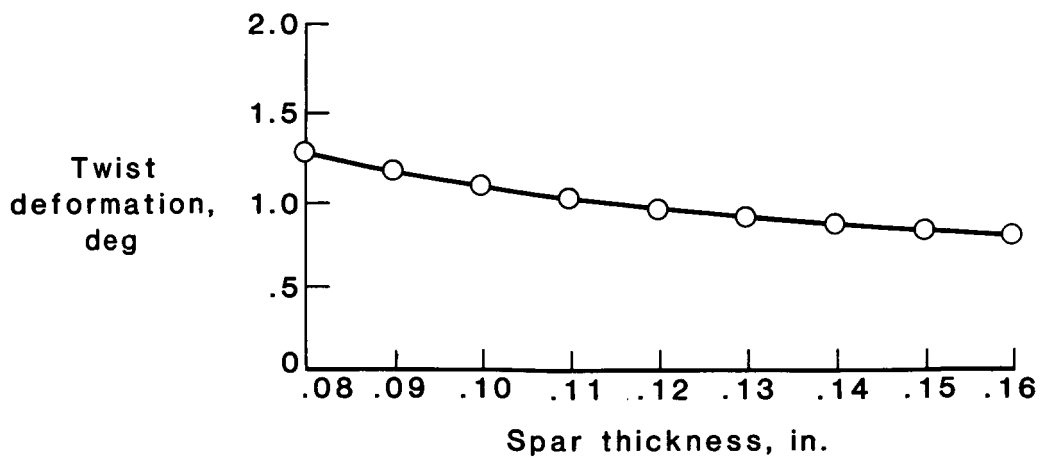


Figure 8. Twist deformation as function of spar thickness for titanium-spar design.

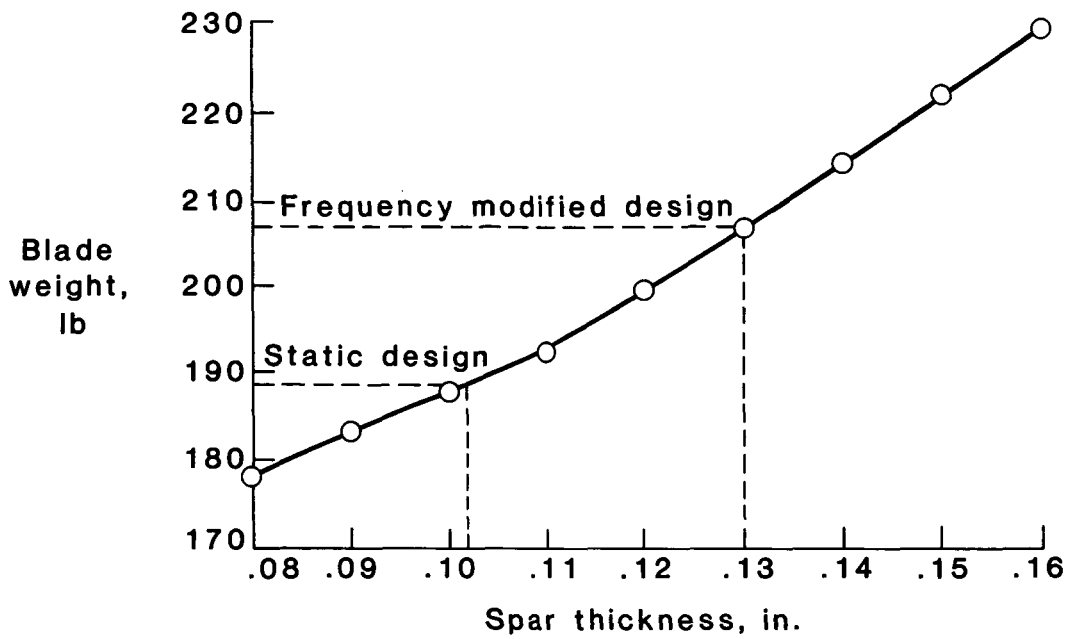


Figure 9. Blade weight as function of spar thickness for titanium-spar design.

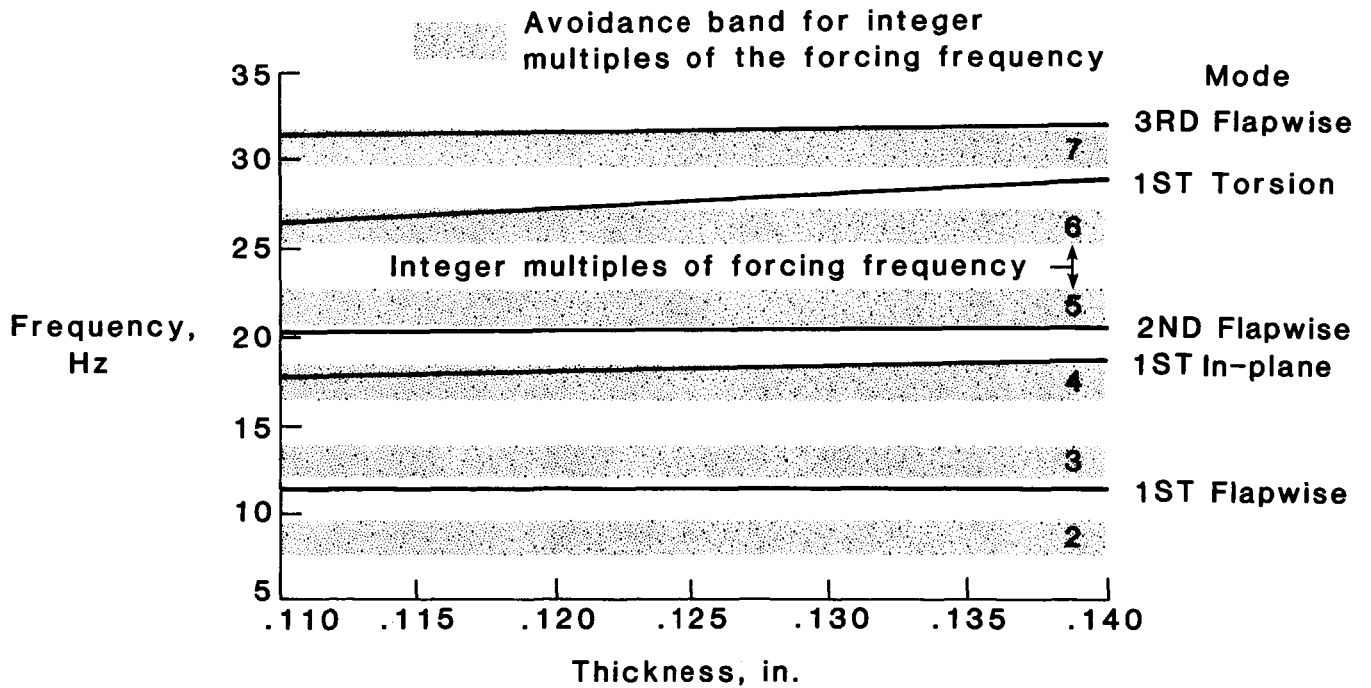


Figure 10. Natural frequencies as function of spar thickness for titanium-spar design.

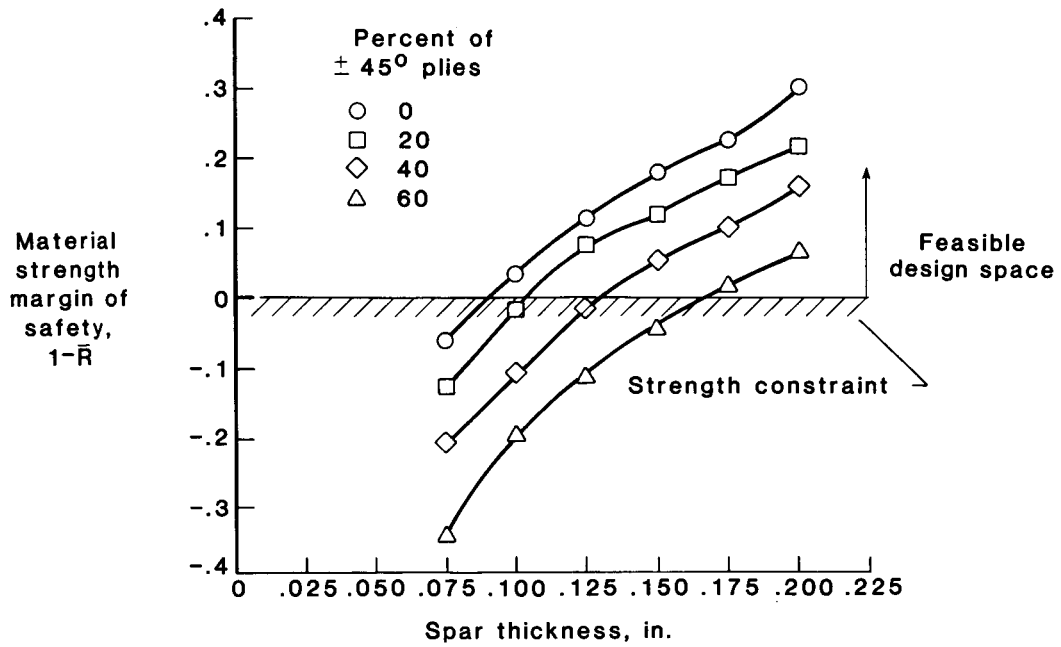


Figure 11. Material strength margin of safety as function of laminate thickness and ply orientation for single composite-spar design.

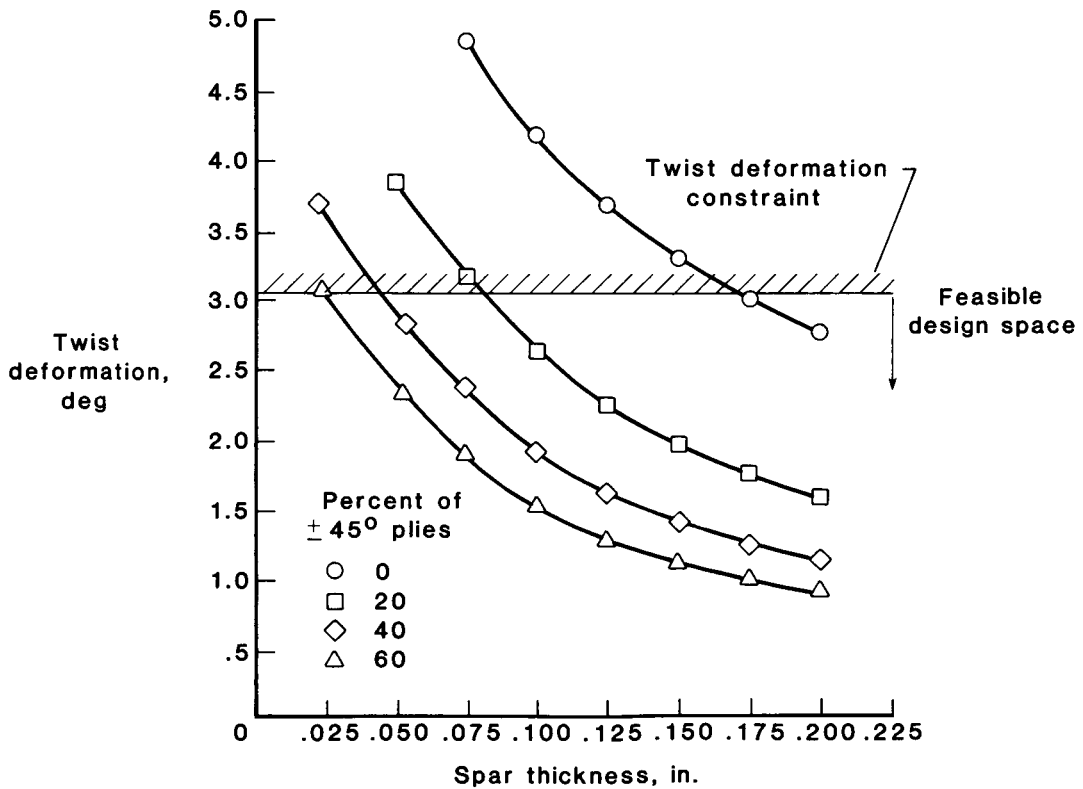


Figure 12. Twist deformation as function of laminate thickness and ply orientation for single composite-spar design.

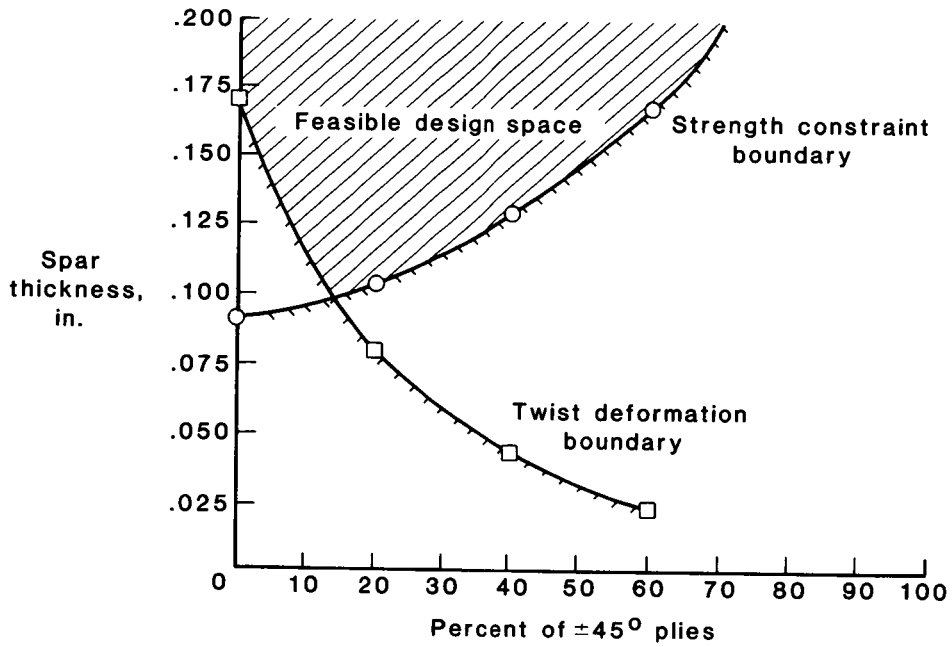


Figure 13. Feasible design space for single composite-spar design.

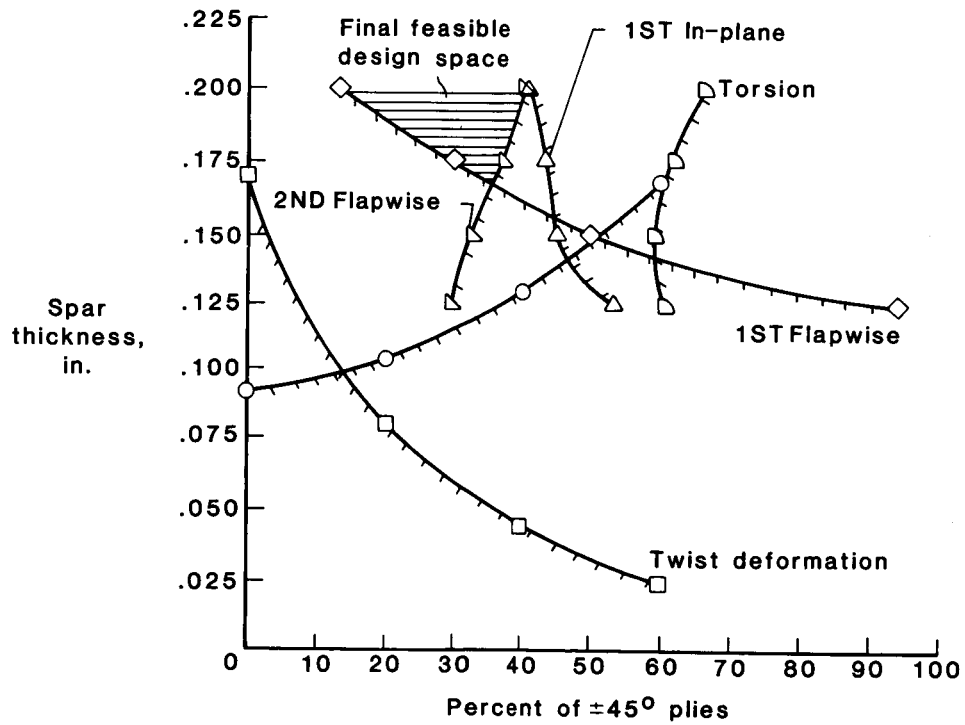


Figure 14. Feasible design space for single composite-spar design with frequency constraints.

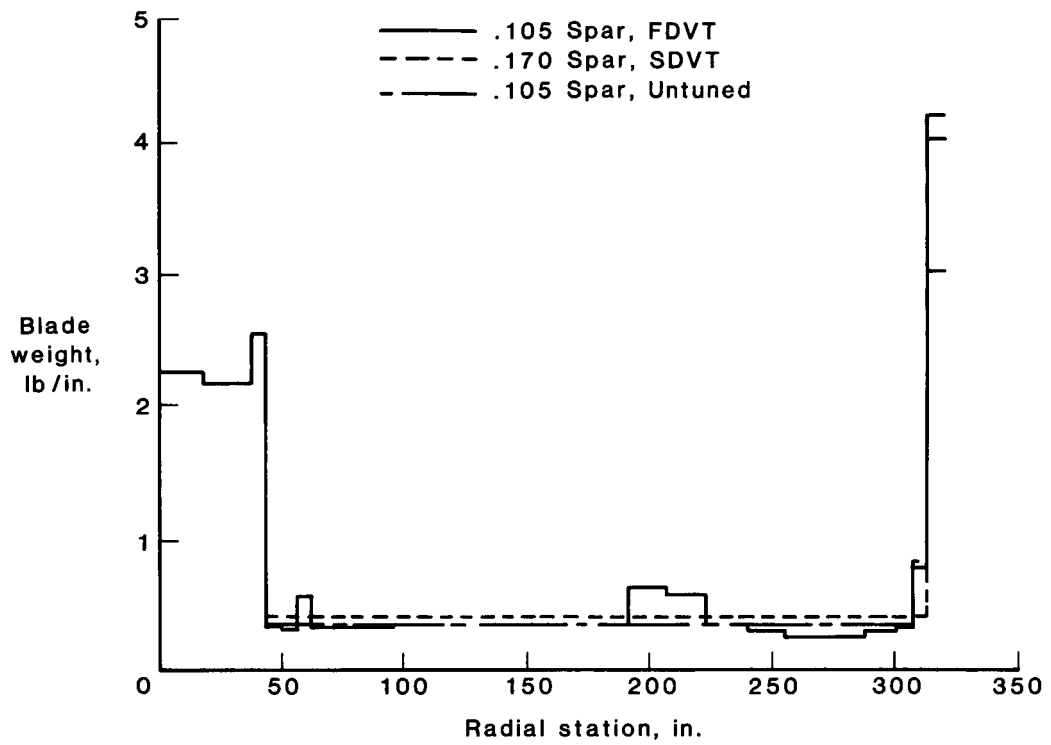


Figure 15. Weight distribution of single composite-spar design.

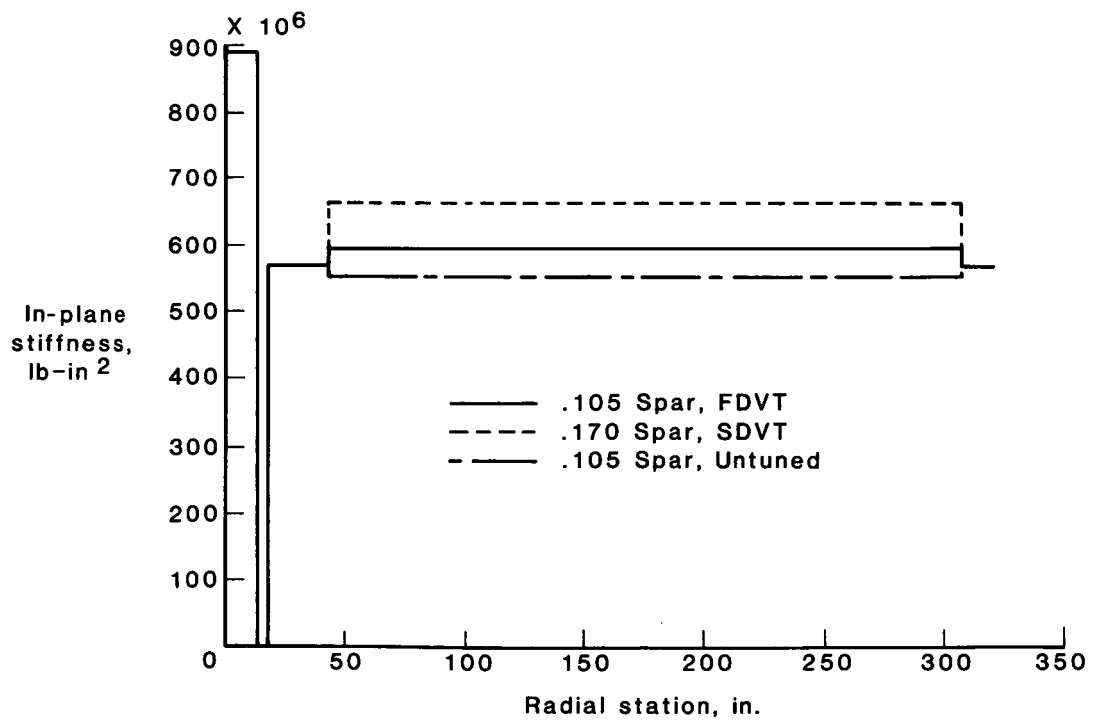


Figure 16. Edgewise stiffness distribution of single composite-spar design.

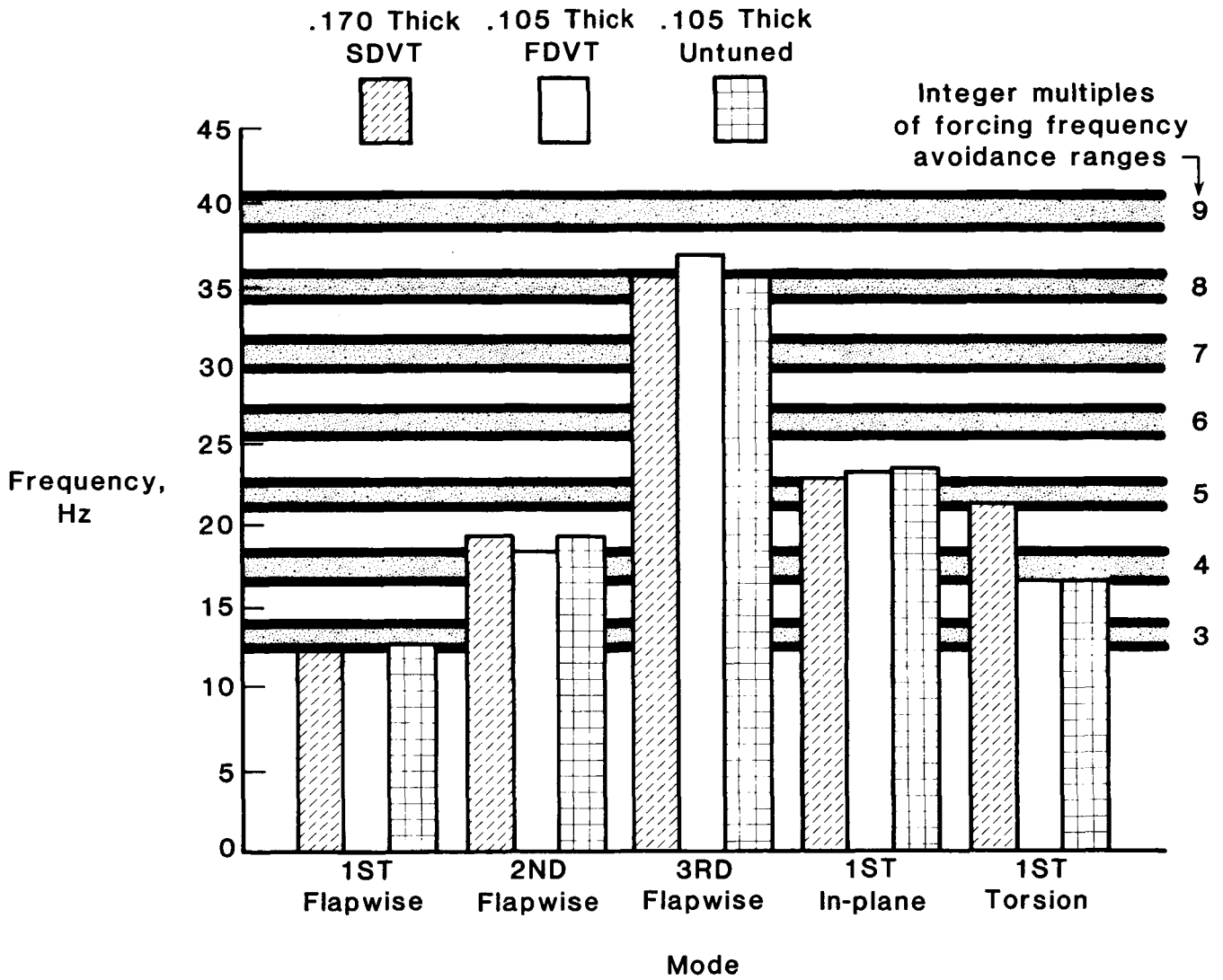


Figure 17. Natural frequencies of single composite-spar design.

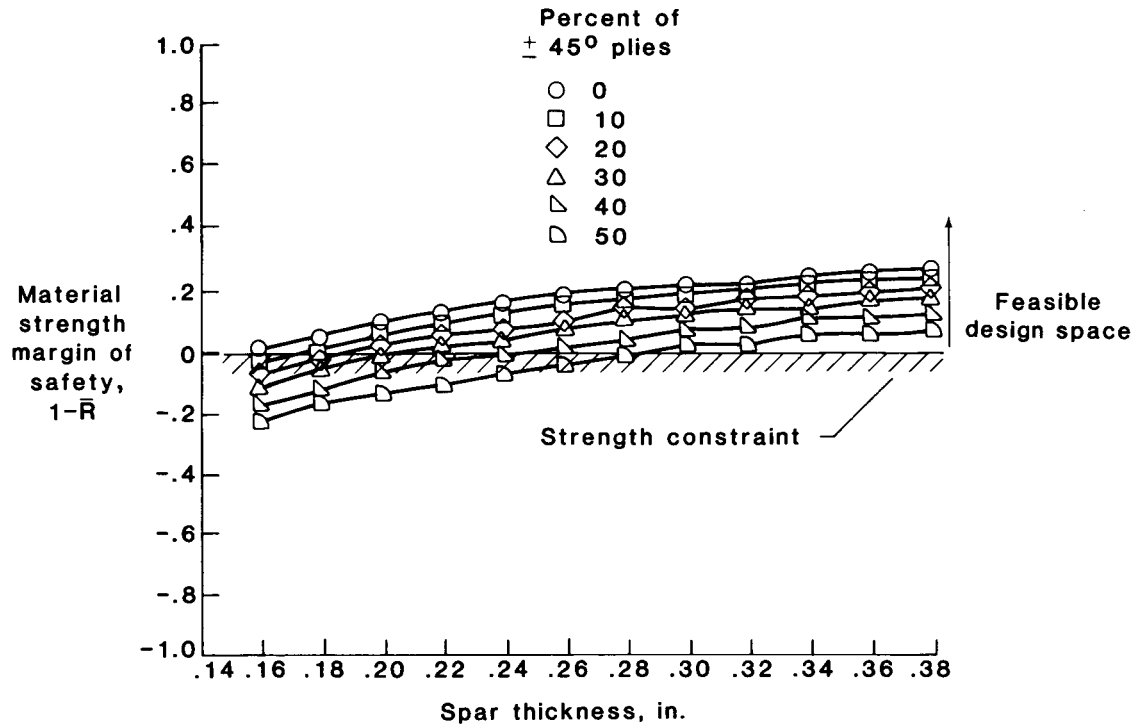


Figure 18. Material strength margin of safety as function of laminate thickness and ply orientation for multiple composite-spar design.

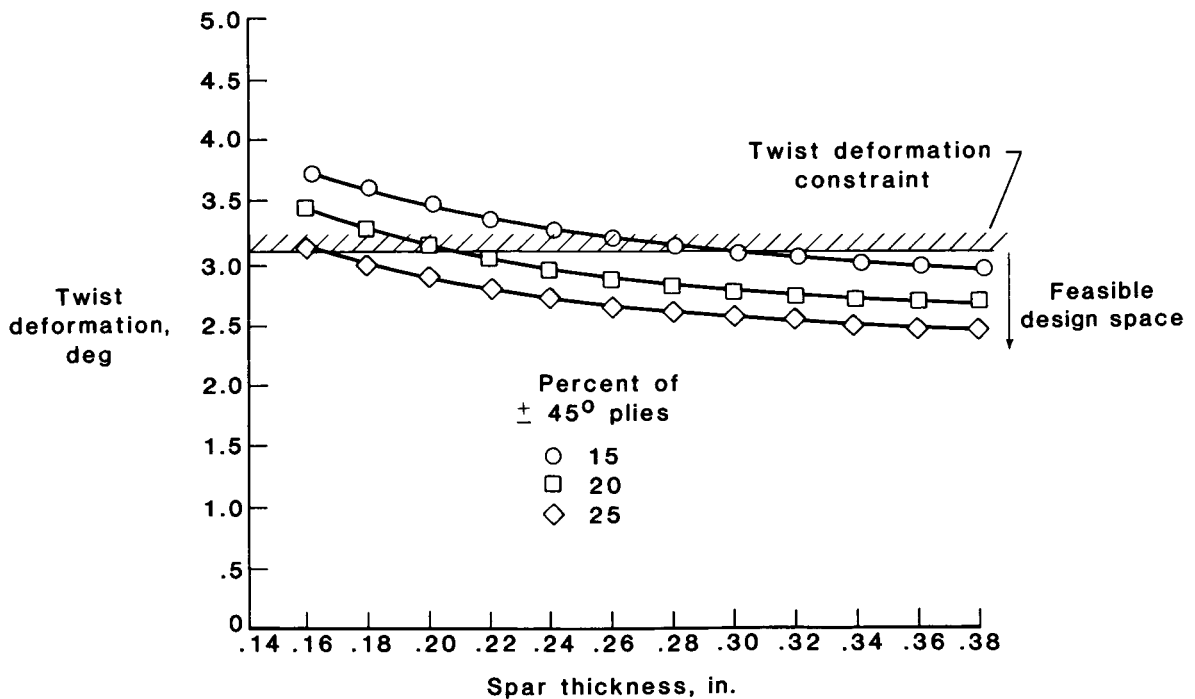


Figure 19. Twist deformation as function of laminate thickness and ply orientation for multiple composite-spar design.



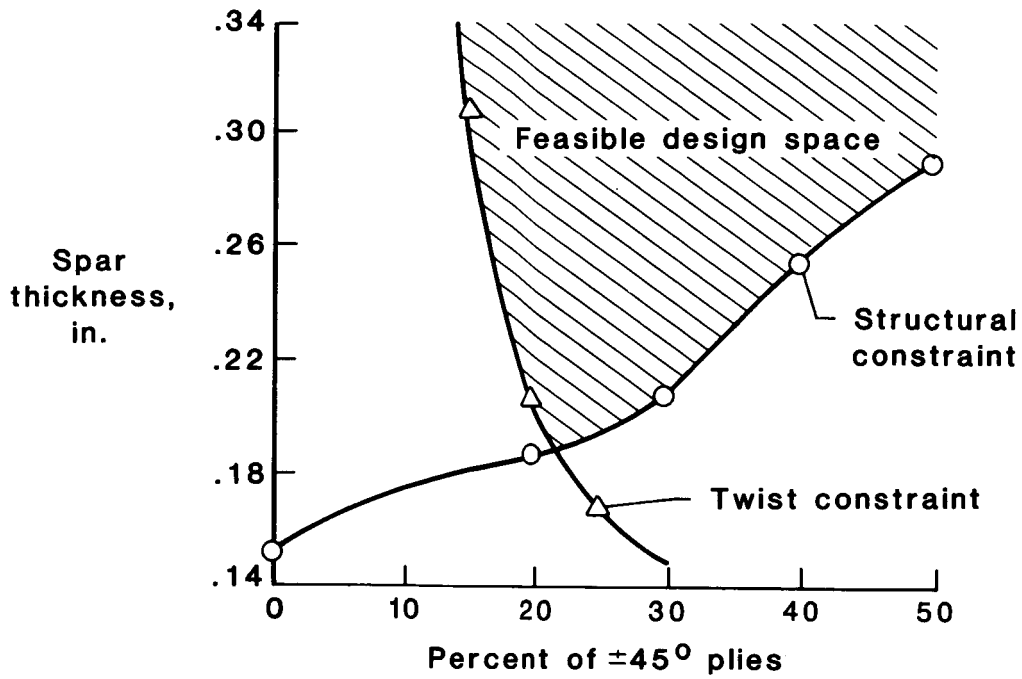


Figure 20. Feasible design space for multiple composite-spar design.

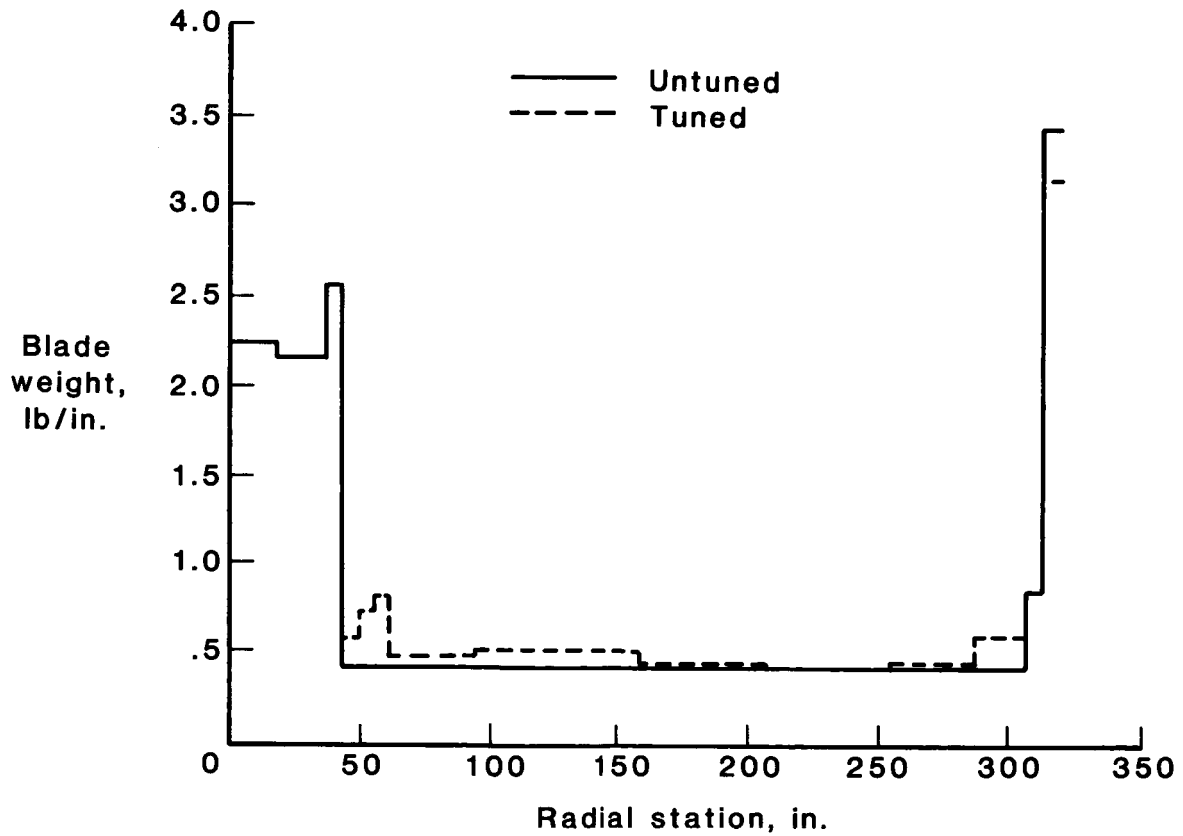


Figure 21. Weight distribution of multiple composite-spar design.

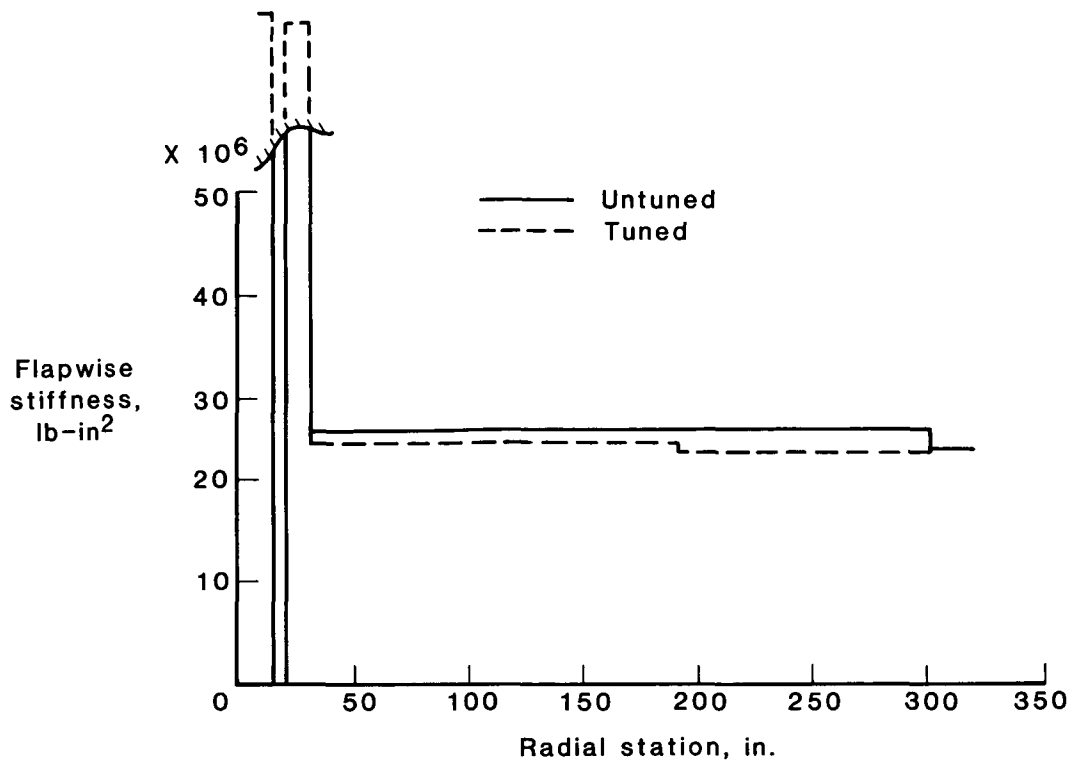


Figure 22. Flapwise stiffness distribution of multiple composite-spar design.

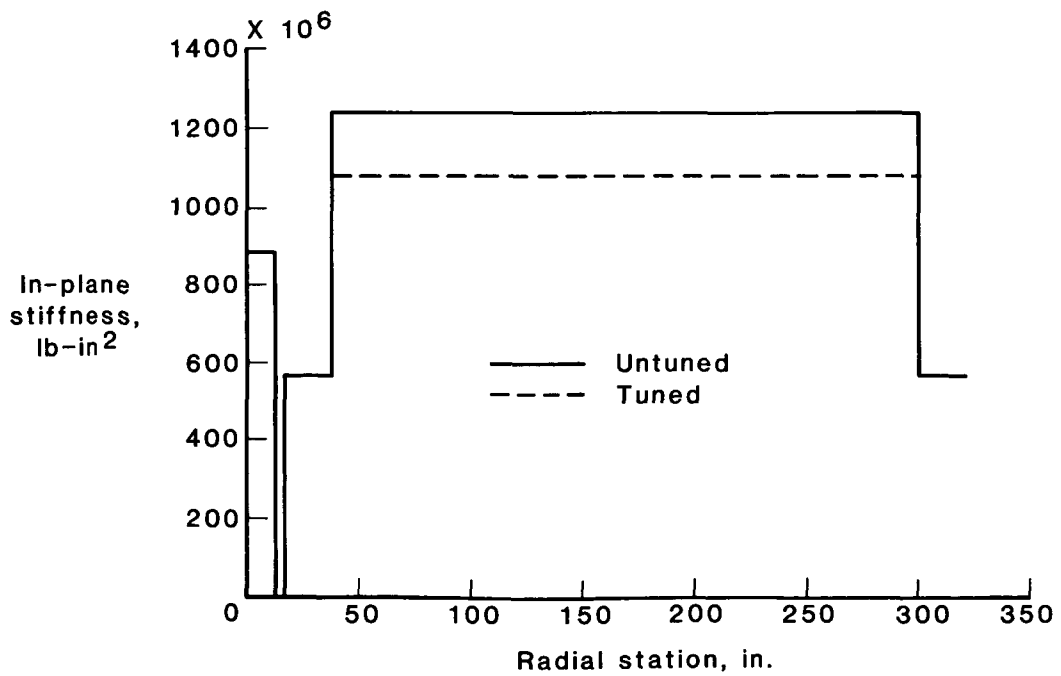


Figure 23. In-plane stiffness distribution of multiple composite-spar design.

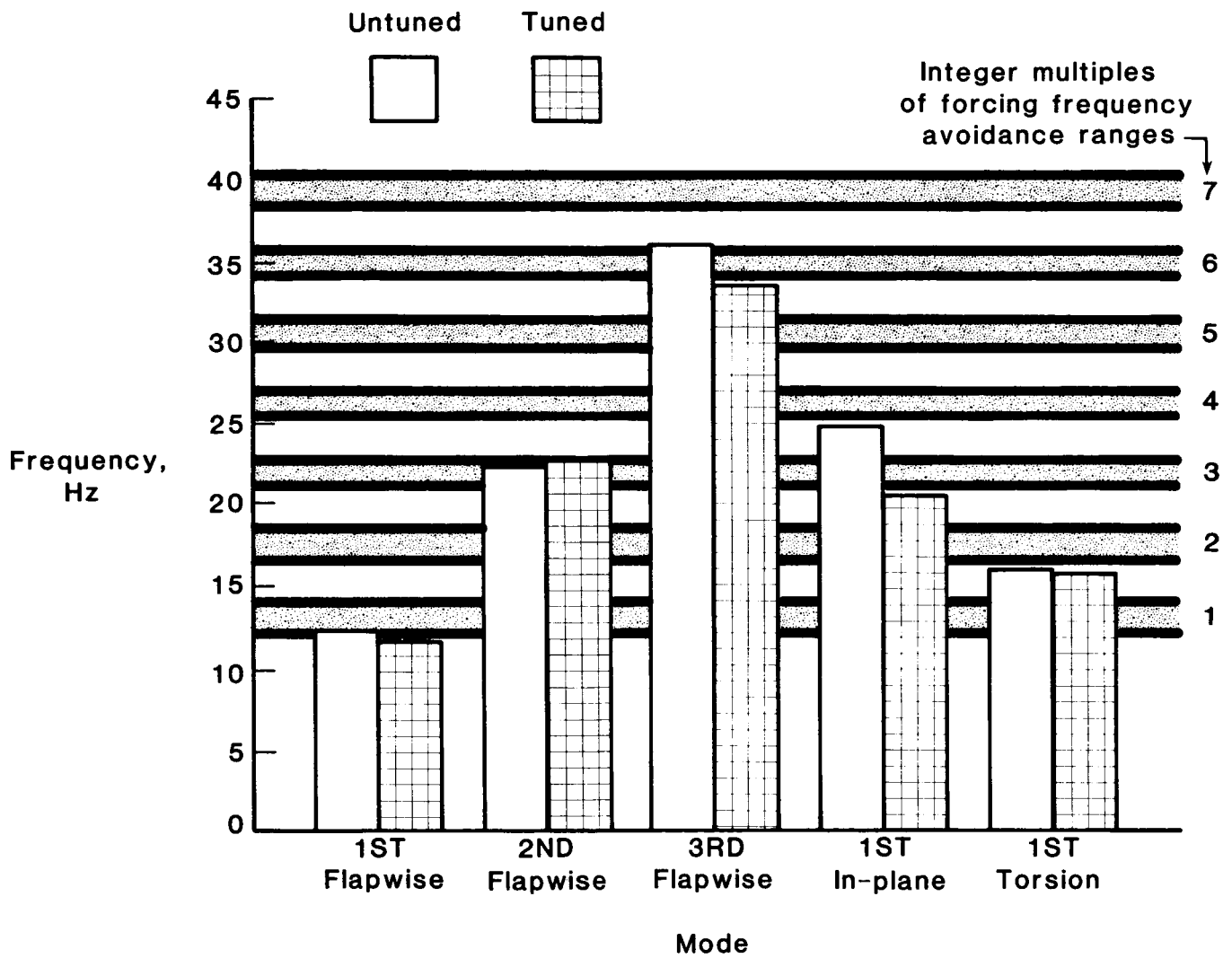


Figure 24. Natural frequencies of multiple composite-spar design.



## Report Documentation Page

<b>1. Report No.</b> NASA TP-2730 AVSCOM TM 87-B-6	<b>2. Government Accession No.</b>	<b>3. Recipient's Catalog No.</b>	
<b>4. Title and Subtitle</b> Preliminary Structural Design of Composite Main Rotor Blades for Minimum Weight		<b>5. Report Date</b> July 1987	
		<b>6. Performing Organization Code</b>	
<b>7. Author(s)</b> Mark W. Nixon		<b>8. Performing Organization Report No.</b> L-16310	
		<b>9. Performing Organization Name and Address</b> Aerostructures Directorate USAARTA-AVSCOM Langley Research Center Hampton, VA 23665-5225	
<b>12. Sponsoring Agency Name and Address</b> National Aeronautics and Space Administration Washington, DC 20546-0001 and U.S. Army Aviation Systems Command St. Louis, MO 63120-1798		<b>10. Work Unit No.</b> 505-63-51-01	
		<b>11. Contract or Grant No.</b>	
<b>13. Type of Report and Period Covered</b> Technical Paper		<b>14. Army Project No.</b> 1L162209AH76	
		<b>15. Supplementary Notes</b> Mark W. Nixon: U.S. Army Aerostructures Directorate, USAARTA-AVSCOM.	
<b>16. Abstract</b> <p>A methodology is developed to perform minimum-weight structural design for composite or metallic main rotor blades subject to aerodynamic performance, material strength, autorotation, and frequency constraints. The constraints and load cases are developed such that the final preliminary rotor design will satisfy U.S. Army military specifications. In addition, the methodology uses design variables which can take advantage of the versatility of composite materials. A minimum-weight design is first developed subject to satisfying the aerodynamic performance, strength, and autorotation constraints for all static load cases. The minimum-weight design is then dynamically tuned to avoid resonant frequencies occurring at the design rotor speed. With this design methodology, three rotor blade designs were developed based on the geometry of the UH-60A Black Hawk titanium-spar rotor blade. The first design is of a single titanium-spar cross section, which is compared with the UH-60A Black Hawk rotor blade. The second and third designs use single and multiple graphite/epoxy-spar cross sections. These are compared with the titanium-spar design to demonstrate weight savings from use of this design methodology in conjunction with advanced composite materials.</p>			
<b>17. Key Words (Suggested by Authors(s))</b> Composite materials Helicopter Rotor blades Beam analysis Structural dynamics		<b>18. Distribution Statement</b> Unclassified—Unlimited  <p style="text-align: right;">Subject Category 24</p>	
<b>19. Security Classif.(of this report)</b> Unclassified	<b>20. Security Classif.(of this page)</b> Unclassified	<b>21. No. of Pages</b> 26	<b>22. Price</b> A03